

# Distributed Measurements of the Penetration Loss of Railroad Cars

Martin Lerch<sup>\*†</sup>, Philipp Svoboda<sup>†</sup>, Stephan Ojak<sup>‡</sup>, Markus Rupp<sup>†</sup> and Christoph Mecklenbräuker<sup>†</sup>

<sup>\*</sup>Christian Doppler Laboratory for Dependable Wireless Connectivity for the Society in Motion

<sup>†</sup>Institute of Telecommunications, TU Wien, Austria

<sup>‡</sup>ÖBB Technische Services GmbH, Austria

mleerch@nt.tuwien.ac.at

**Abstract**—The mobile cellular service coverage of nomadic users in the context of high speed vehicular scenarios, e.g., railroad trains, is challenging. Energy saving efforts of the past years have lead to substantially increased vehicle penetration losses, e.g., by metal shielded windows. As a result providing coverage into railroad cars is an emerging topic for optimization efforts, either based on network deployment or on railroad car materials. The quality of these efforts rely heavily on the understanding of the vehicle penetration loss and its angular dependency. In this paper we present a distributed measurement methodology and setup allowing for measuring the penetration loss of railroad cars. We validate the feasibility of the methodology in a real world measurement campaign in Austria. There, we compare two different car configurations, standard and prototypical, at 800—2600 MHz for azimuthal angles of arrival of 0—60 degree. The comparison of the two configurations shows a substantial lower penetration loss of the prototypical setup due to windows with alternative material treatment.

## I. INTRODUCTION

Mobile service coverage for nomadic users on board trains remains a challenging scenario for cellular technologies. There are multiple reasons to this, e.g., fast hand-overs, high local cell loads and in general the high Vehicle Penetration Loss (VPL). The VPL in public transportation is high due to metal coating applied to the windows as an isolation to the infrared part of sunlight. This metal coating typically results in an attenuation of mobile signals of up to 40 dB. The same applies for modern electric cars due to energy saving efforts. The additional attenuation caused by VPL in combination with the rural, low populated areas highways and railroads are passing, results in a very low general service quality.

As a consequence different solutions have been studied to improve the level of mobile signal strength inside the railroad cars. The current studies are split into two main sets [1]. The first set deals with the optimization of the deployed cells around the track of the train. Small cells in rural areas are an expensive investment, especially considering the low frequency of use, e.g., railroads. A solution is to provide cellular coverage with relay antennas deployed over multiple locations along the track. The system repeats the signal of the master node at each relay providing a continuous high level of signal strength along the repeater chain. The theoretical peak capacity of the cell remains unchanged. Relay deployments along railroads are still costly due to the small cell size and

the location close to the track, resulting in an obtuse Angle of Arrival (AoA) at the railroad car.

The second set focuses on modifications of the VPL itself. Recent railroad cars have lowered the VPL from former 60 dB as far as 20 dB by reducing the thickness of the metal coating. Still the remaining VPL exceeds typical indoor penetration loss values mobile operators use for planning their networks. An active solution is the deployment of repeaters in railroad cars. The system uses an outdoor antenna, an amplifier and an indoor leaky cable distribution to lower the VPL to virtually zero [2], [3]. The passive solution is using a modified metal coating on the window using regular structures acting as small antennas allowing the electromagnetic waves to pass at low levels of VPL, see [4].

A smart combination of these two approaches, namely a densification of the deployment using repeater chains along the track and a reduction of the VPL by modifications of the railroad cars, is important. A major missing link to combine these two improvement strategies, is a better understanding on the angular impact to VPL. In other words a measurement of the penetration loss of the cabin windows for different AoAs.

## Related Work

There is only limited literature available on measurements performed in the context of railroad cars. In [5] the authors measured the radio channel properties outside the railroad cars, this allows a characterization of channel parameters. In [6] the authors used an antenna setup in the cabin and on the rooftop of a railroad car measuring channel parameters such as the Doppler profile. The authors of [7] focused on subway cars moving in tunnels and the according effects of wave guiding.

Literature in the context of indoor penetration loss for buildings is available for various materials and scenarios. A large collection of results is presented in the ITU report P.2346 relating to building entry loss. The report also analyzes the elevation angle as one component of the measurement. In [8] the authors have specified a measurement methodology to measure the penetration loss of building walls, e.g., stone or glass, at 5 GHz. Results on VPL measured for cars with different directions of illumination is presented in [9]. The results are close to values derived from simulations and range between 3 and 20 dB.

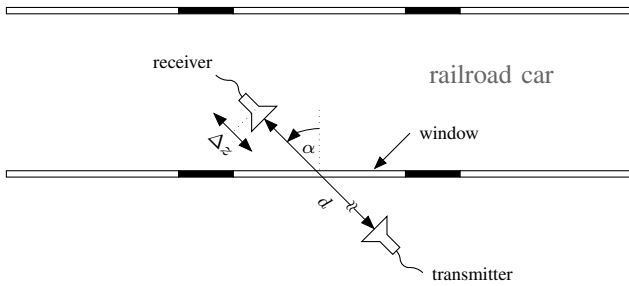


Fig. 1. Measurement geometry to measure the VPL at different AoAs.

All the previous measurement work reflects very closely the scenario it was recorded in. These results can be applied in similar scenarios only and not generalized further.

### Contribution

In this work we have derived a methodology for repeatable and controllable measurements of the VPL of railroad cars. The setup is designed to measure solely the impact of the VPL without considering a specific scenario, e.g., test drive. We test our measurement setup in a campaign comparing two railroad cars equipped with different types of windows. In this campaign we measured various radio frequencies used for cellular mobile communication in Europe.

## II. MEASUREMENT METHODOLOGY

In order to fairly compare the VPL of different railroad cars at different frequencies and different AoAs we do measurements according to the geometry illustrated in Figure 1. Thereby, we evaluate the angle dependency of the VPL by moving both, the transmit antenna and the receive antenna along semicircles with center point at the center point of a train window. A constant distance between the transmitting and the receiving antenna grants a constant Free-Space Path Loss (FSPL). Furthermore, the impact of the antenna patterns on the Line-Of-Sight (LOS) component is fixed.

In the railroad car, we combat the impact of small-scale fading due to multipath propagation by spectral averaging (see Eq. (4)) and spatial averaging along the connecting line of the antennas (see Figure 1). In our measurements, the linear guide used for moving the antenna inside the cabin allows for an averaging length of  $\Delta z=0.72$  m. Thereby, the variation of the FSPL decreases with increasing distance between the antennas. For our measurement setup the average distance between the antennas is 4.66 m. The resulting difference in FSPL between the highest and the smallest distance is approx. 1.3 dB. In our measurements we eliminate this effect by performing a calibration measurement that will be explained subsequently.

In order to focus on the impact of the train rather than the impact of the actual measurement scenario we place the railroad car under test in a low scattering environment similar to an anechoic chamber. Furthermore, we avoid significant reflections from the ground by

- choosing a measurement location without a platform.
- using an outside antenna with a narrow vertical pattern.

- keeping the distance from the outside antenna to the train as small as possible.

### Determination of the VPL

Averaging the received power obtained at different receiver positions along the connecting line of the antennas yields the average loss

$$P_{\text{TX}} - \overline{P_{\text{RX}}}(\alpha, f) = \overline{L_{\text{FS}}}(f) + L_{\text{setup}}(f) + \overline{L_{\text{VPL}}}(\alpha, f) \quad (1)$$

between the transmitter port and the receiver port. Besides the average VPL  $\overline{L_{\text{VPL}}}$  this loss also includes the average FSPL  $\overline{L_{\text{FS}}}(f)$  and the loss of the setup  $L_{\text{setup}}(f)$  that comprises the gains of the antennas and the cable losses. The measured loss allows for a relative comparison of, e.g., different kinds of train windows. In order to obtain the absolute value  $\overline{L_{\text{VPL}}}(\alpha, f)$  of the VPL, we perform a calibration measurement in an anechoic chamber. Thereby, we perform exactly the same measurement as with the train under test and obtain the loss of the measurement setup and the FSPL:

$$P_{\text{TX}} - \overline{P_{\text{RX,ref}}}(f) = \overline{L_{\text{FS}}}(f) + L_{\text{setup}}(f). \quad (2)$$

Alternatively, the absolute value of the VPL can also be obtained through a calibration measurement with the receive antenna mounted at the exterior of the train [9].

### Instrumentation Setup

In the following we will outline the selected setup for the measurements. This setup is based on several assumptions. First we target to measure long-distance high-speed passenger trains. A typical train consists of several passenger railroad cars, each with 20–30 m of length. The physical size of the setup cannot be neglected and has to be accounted for. Considering the usage of a network analyzer to perform the measurements of the VPL the length of cables connecting the transmitter and the receiver needs to be considered in the link budget. In our specific case the calculated link budget showed the need to use additional amplifiers for compensation of this cable loss. Typical measurement amplifiers are narrowband. As our frequencies of interest span a range from 800–2600 MHz, this setup would require a number of different amplifiers.

Derving the VPL does not depend on the phase of the received signal. Therefore, we adapted our setup into a distributed configuration, replacing the network analyzer with two devices, namely, a arbitrary waveform generator and a spectrum analyzer. These two devices allow for flexibility in tuning the receiver sensitivity. The only constraint in this setup is a carrier frequency synchronization between transmitter and receiver. This can be achieved with rather low requirements, e.g., via a 10 MHz port. A combined operation is granted by linking the transmitter unit with the receiver unit via a LAN connection.

### Transmit signals

In our measurements we consider Orthogonal Frequency Division Multiplexing (OFDM) signals similar to 20 MHz

TABLE I  
MEASUREMENT PARAMETERS

Measurement location	Prinzersdorf railway station, Austria
Date	23.4.2016
Center frequencies $f_c$	800 MHz, 1.8 GHz, 2.1 GHz, 2.6 GHz
Angles $\alpha$	$0^\circ, 15^\circ, 30^\circ, 45^\circ, 60^\circ$
Antenna distance $d$	4.3 m—5.02 m
Polarization	vertical
Transmit antenna	Poynting OMNI-69 [10]
Signal source	Rohde & Schwarz SMU 200A
Transmit signal	OFDM, 1200 subcarriers @ $\Delta f=15$ kHz
Receive antenna	Aaronia Hyperlog 6080 [11]
Receiver	Keysight N9020A

3GPP Long Term Evolution (LTE) downlink signals<sup>1</sup>. Unlike in the case of LTE, the signal is only used to estimate the received signal power. This allows for certain simplifications in the implementation and in the hardware setup. By continuously transmitting the same OFDM symbol, a cyclic prefix is not necessary. The transmit signal  $x(t)$  then simplifies to a sum of  $N_s$  orthogonal sinewaves modulated with random symbols  $a[k]$  chosen from a Quadrature Phase-Shift Keying (QPSK) signal constellation:

$$x(t) = \sum_{\substack{k=-N_s/2 \\ k \neq 0}}^{N_s/2} a[k] e^{j\Delta f k t} \quad -\infty < t < \infty. \quad (3)$$

This approach allows for a free-running transmitter and therefore time-synchronization of the transmitter and the receiver is not necessary.

#### Power estimation

At the receiver side we estimate the received power by sampling the received signal over a duration of  $N=100$  OFDM symbols. The received signals are then processed offline. Thereby, we demodulate the received signal symbol-per-symbol and coherently average the received symbols  $Y_{k,n}$  over time before we estimate the received power

$$\hat{P}_{RX} = \sum_{\substack{k=-N_s/2 \\ k \neq 0}}^{N_s/2} \left| \frac{1}{N} \sum_{n=0}^{N-1} Y_{k,n} \right|^2 \quad (4)$$

as the sum over all  $N_s$  subcarriers. Thereby, on the one hand, we can arbitrarily increase the sensitivity of the power estimation by increasing the number  $N$  of OFDM symbols considered in the average. On the other hand, this approach requires the receiver to be carrier frequency synchronized to the transmitter.

### III. MEASUREMENT

In this measurement campaign we applied the methodology introduced in Section II for measurements with railroad cars of a complete train. The train under test was a Railjet operated by the Austrian Federal Railways (OEBB). In this measurement

<sup>1</sup>As in 20MHz LTE we transmit  $N_s=1200$  subcarriers with a subcarrier spacing of  $\Delta f=15$  kHz. The resulting signal bandwidth is approx. 18 MHz.

campaign we compared two different configurations of railroad cars, configuration one uses standard windows, while configuration two uses prototypical windows [4]. Thereby, both measurements were conducted at window five in the middle of a economy type railroad car (see Figure 2).

The measurements were performed on an unused sidetrack close to the railroad station of Prinzersdorf, Austria. The surrounding features a flat terrain and the corresponding absence of scattering objects. This eliminates unwanted contributions from any multipath components, e.g., diffracted, refracted, and scattered waves.

Furthermore, assuming all possible sources of interference being located outside the train, the contribution of our transmit signal to the total received power dominates the interference. Note that any signal received at the inside of the train is attenuated by the VPL.

#### Angular Dependent Setup

The planned deployment of base stations for increased railroad coverage is close to the center of the track, e.g., 5 — 15 m. Such close distance between base station and rail track results in a predominantly grazing angle of arrival with respect to the window's glass surface. Therefore, the second parameter we analyzed in our measurement setup was the dependency on the AoA. We measured angles from  $0^\circ$  (Line of Sight perpendicular to the glass surface) to  $60^\circ$  (grazing angle). Note that we assume angularity symmetric attenuation properties of the window's glass structure and mirrored angles from  $-60^\circ$  to  $0^\circ$  to experience identical attenuation.

#### Outside Unit

This unit was setup with a uniform broadband transmit antenna with a gain of 3 dBi, see Figure 2b and [10]. The uniform pattern was chosen to illuminate the whole cabin from the outside of the train. A high gain antenna is narrowband and not suitable for this measurement. The outside antenna was mounted fixed on a tripod in a distance of 4 m from the center of the window under test. The total distance between the antennas was chosen to be larger than  $2D^2/\lambda$  for 2.6 GHz and  $D=0.48$  m.

#### Inside Unit

At the inside unit, we used a broadband log-periodic antenna with a gain of 6 dBi, see Figure 2a. The antenna pattern of this antenna is comparable to a normal mobile handset, e.g., radiation pattern in one direction. Polarization wise both antennas have been aligned with the same vertical polarization. The main lobe of the antennas is aligned using laser measurements. This was used to fix the measurement point in the middle of the window under test as well as leveling the antenna heights. The inside antenna is moved from 30 cm minimum distance from the measurement point, linearly to approx. 100 cm with an automatic operated linear guide.



Fig. 2. Measurement setup: (a) The receive antenna inside the train is moved along the connecting line to the transmit antenna using a linear guide. (b) The transmitter is located outside the train.

### Procedure

Given an eight hour time limitation of the measurement only four dedicated frequencies have been selected for measurement. At each frequency we transmitted the same signal with a bandwidth of 18 MHz. The frequencies measured cover all main mobile technologies and correspond or are close to the Universal Mobile Telecommunications System (UMTS) bands and the LTE bands B20, B3 and B7.

The following list gives a summary of the steps for the measurement:

- Select current measurement angle: 0, 15, 30, 45, 60,
- Align inside and outside unit,
- Select current frequency: 800, 1800, 2100, 2600,
- Measure signal power at 20 equally spaced positions of the receive antenna.

A complete cycle at a given angle took 30 min. This set of measurement was repeated three times, one time for each window configuration and one time in an anechoic chamber to provide for a reference level. A summary of all measurement parameters is given by Table I.

### IV. RESULTS

In the following we present and discuss the results collected in the Railjet measurement campaign. Figure 3a shows the raw received signal power  $P_{RX}$  for an angle of arrival of  $\alpha=0^\circ$  and for the three different scenarios: Railjet with standard configuration, Railjet with prototype configuration and the reference measurement in the anechoic chamber. The small confidence intervals, denoted as bars at each measurement point, support our choice of averaging in space. The values of absolute power are well above our noise floor.

The comparison with the results of the reference measurement performed in the anechoic chamber directly yields the penetration loss  $L_{VPL}$  shown in Figure 3b. Thereby, the standard window shows a relative constant attenuation for the different frequency points, especially if the confidence

intervals are considered. The mean ranges from 15—17 dB. The prototypical window configuration of the railroad car has a strong frequency dependency. The attenuation values range from a maximum of 12 dB down to as low as 3 dB.

In Figure 4 we discuss the results for each window as a function of the angular setting. Each window configuration has a set of curves, solid for prototype and dashed for the standard window. The set consists of four curves one for each frequency. The result shows only very weak angular dependency of the VPL in nearly all of the setups. In the prototype configuration the 800 MHz measurement has a strong drop of the VPL at  $30^\circ$ . We assume that this is due to the structure applied to the windows, it might change its properties for different angles of arrival.

### V. CONCLUSIONS

In this paper we introduced a distributed measurement methodology for measuring the VPL in an controlled and repeatable fashion at a wide range of frequencies. The setup is especially tailored for the need of railroad scenarios in terms of physical size of the site as well as used frequencies and bandwidth. The setup offers improved SNR by averaging an LTE like 20 MHz signal and minimized effects of small scale fading by spatial and spectral averaging. It can operate in a fully distributed fashion, e.g., using Rubidium frequency normals.

We realized an initial test setup based on the methodology and conducted a measurement campaign. Here, we measured the VPL of a Railjet railroad car for a frequency range from 800—2600 MHz for two different window configurations. The standard configuration has a VPL in the order of 17 dB. The configuration featuring windows with specially treated surfaces have a VPL from 10 dB down to as low as 3 dB. Both configurations show only minor angular dependency of the VPL.

The measurement campaign verified the feasibility of the methodology. This will allow to collect comparable measure-

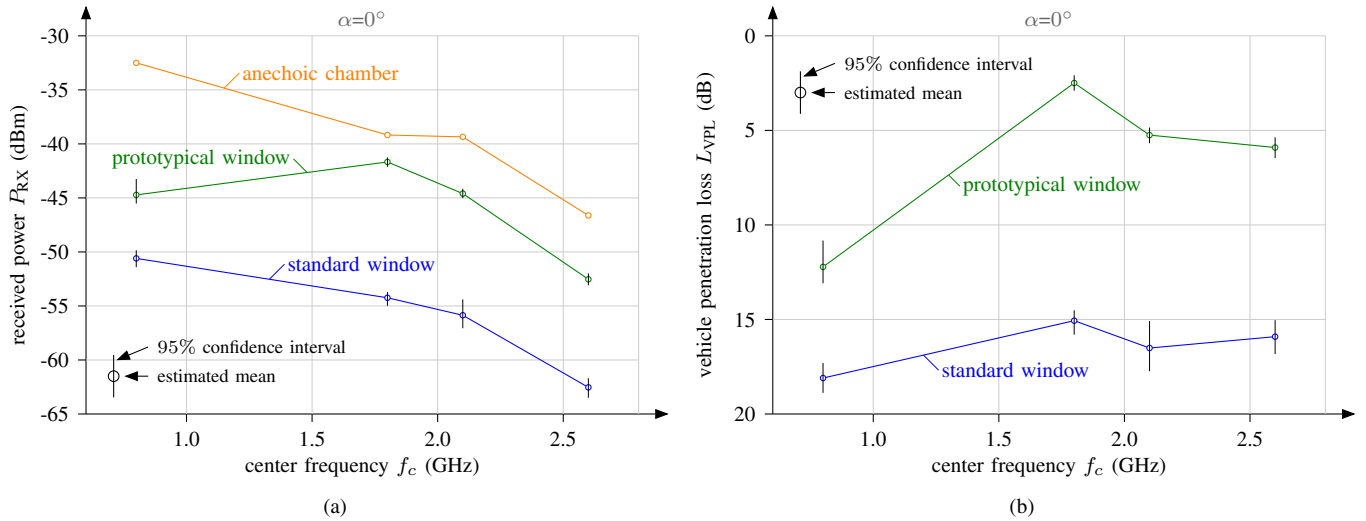


Fig. 3. Measurement results for  $\alpha=0^\circ$ : (a) Received power for both kinds of train windows and for the reference measurement in the anechoic chamber. The results obtained in the anechoic chamber reflect the frequency-dependency of the setup. (b) Vehicle penetration loss for both kinds of windows after calibration using the results obtained in the anechoic chamber.

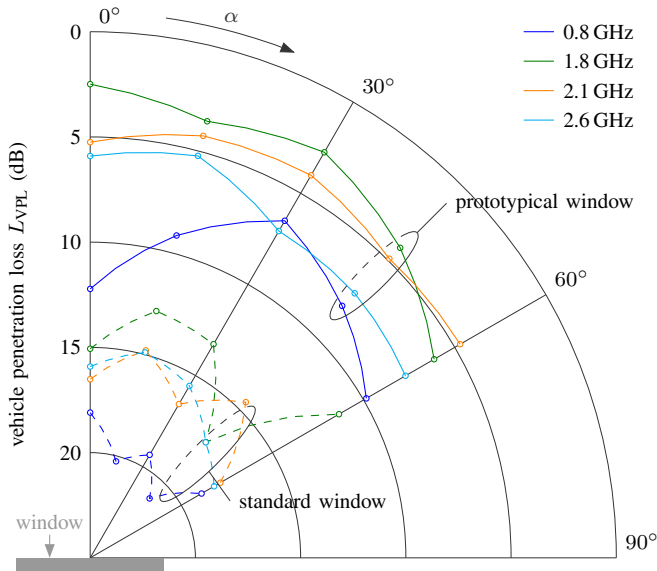


Fig. 4. Measurement results for different AoAs and different frequency bands.

ments for different types of railroad cars as well as different types of configurations, allowing for further optimization in simulations. Open further topics are the impact of parameters such as polarization and elevation, and an extension of this method towards other types of vehicles.

#### ACKNOWLEDGMENTS

This work has been funded by National Railways of Austria - ÖBB, the ITC, TU Wien and A1 Telekom Austria AG. The financial support by the Austrian BMWFV and the National Foundation for Research, Technology and Development is gratefully acknowledged. The research has been co-financed by the Czech GA CR, Project No. 17-18675S and No. 13-38735S, by the Czech Ministry of

Education in the frame of the National Sustainability Program under grant LO1401 and supported by the Austrian FFG, Bridge Project No:850742.

#### REFERENCES

- [1] M. K. Müller, M. Tarantetz, and M. Rupp, "Providing Current and Future Cellular Services to High Speed Trains," *IEEE Communications Magazine*, Oct. 2015.
- [2] T. Berisha, P. Svoboda, S. Ojak, and C. Mecklenbräuer, "Cellular Network Quality Improvements for High Speed Train Passengers by on-board Amplify-and-Forward Relays," in *13th International Symposium on Wireless Communication Systems*, Poznan, Poland, Sep. 2016.
- [3] —, "SegHyPer: Segmentation- and Hypothesis based Network Performance Evaluation for High Speed Train Users," in *IEEE International Conference on Communications (ICC)*, May 2017.
- [4] L. Mayer, A. Demmer, A. Hofmann, and M. Schiefer, "Metal-coated windowpane, particularly for rail vehicles," Feb. 17 2016, eP Patent App. EP20,140,718,024. [Online]: <https://google.com/patents/EP2984707A1?cl=en>
- [5] F. Kaltenberger, A. Byiringiro, G. Arvanitakis, R. Ghaddab, D. Nussbaum, R. Knopp, M. Bernineau, Y. Cocheril, H. Philippe, and E. Simon, "Broadband Wireless Channel Measurements for High Speed Trains," in *IEEE International Conference on Communications (ICC)*, Jun. 2015.
- [6] T. Zhou, C. Tao, S. Salous, L. Liu, and Z. Tan, "Implementation of an LTE-Based Channel Measurement Method for High-Speed Railway Scenarios," *IEEE Transactions on Instrumentation and Measurement*, vol. 65, no. 1, pp. 25–36, Jan. 2016.
- [7] K. Guan, B. Ai, Z. Zhong, C. F. López, L. Zhang, C. Briso-Rodríguez, A. Hrovat, B. Zhang, R. He, and T. Tang, "Measurements and Analysis of Large-Scale Fading Characteristics in Curved Subway Tunnels at 920 MHz, 2400 MHz, and 5705 MHz," *IEEE Transactions on Intelligent Transportation Systems*, vol. 16, no. 5, pp. 2393–2405, Oct. 2015.
- [8] P. Karlsson, C. Bergljung, E. Thomsen, and H. Borjeson, "Wideband measurement and analysis of penetration loss in the 5 GHz band," in *IEEE 50th Vehicular Technology Conference (VTC1999-Fall)*, Sep. 1999.
- [9] E. Tanghe, W. Joseph, L. Verloock, and L. Martens, "Evaluation of Vehicle Penetration Loss at Wireless Communication Frequencies," *IEEE Transactions on Vehicular Technology*, vol. 57, no. 4, pp. 2036–2041, Jul. 2008.
- [10] All-Band LTE/Cellular Omni-Directional Antenna. (Date last accessed 24-02-2017). [Online]: <http://poynting.tech/product/omni-69/>
- [11] Aaronia HyperLOG 6080. (Date last accessed 24-02-2017). [Online]: <http://www.aaronia.com/products/antennas/HyperLog-6080-Pre-Compliance-Antenna/>